Shear in Surface Gel of Associative Polymer

Alexandra Chestakova, Willie Lau, and Eugenia Kumacheva*

Department of Chemistry, University of Toronto, 80 St. George Street, Toronto, Ontario M5S3H6, Canada

Received August 29, 2003; Revised Manuscript Received March 18, 2004

ABSTRACT: The normal and shear forces between adsorbed layers of telechelic associative polymer poly(ethylene oxide) end-terminated with octadecyl groups have been studied using a surface force balance. The normal forces profiles measured for polymer monolayers and surface gels were similar to those reported for the same polymer in earlier studies. The shear forces between the polymer-covered surfaces were very weak up to compression of ca. 0.27 of the original thickness of the polymer layers, corresponding to the effective friction coefficient $\mu < 0.04$. Weak frictional forces were attributed to osmotic repulsion between poly(ethylene oxide) chains and shear thinning of the gelled polymer. At higher polymer compression the shear forces gradually increased due to compression-forced increase in interpenetration and entanglement of the macromolecules adhering to the two opposite surfaces and interactions between the octadecyl groups. Shear thinning was also observed for long-time shear and for shear velocity v_s exceeding 600 nm/s. For strongly compressed polymer and $v_s < 600$ nm/s the dependence of frictional forces on the shear velocity was weak, caused by a thinning of the interpenetration zone between the sheared polymer layers and/or a transition of the slip plane to the polymer−substrate interface.

Introduction

Water-soluble polymers bearing hydrophobic groups find applications in food, paint, paper, cosmetic, and pharmaceutical industries[1,2] due to their intrinsic ability to undergo thermoreversible association in aqueous solutions. The mechanism of association is best understood for telechelic polymers: linear hydrophilic chains bearing hydrophobic groups at both ends. Following increase in polymer concentration in solution, these molecules generally undergo a sequence of structural transformations: from the isolated macromolecules to micelles with a hydrophobic core and a hydrophilic corona, then to micellar aggregates, and finally to a physical network formed by the interconnected micelles.[3]

Network formation leads to a great increase in solution viscosity, even when polymer concentration does not exceed several weight percent. Because of the physical nature of association, viscosity of the system shows a strong dependence on the shear rate, $\dot{\gamma}$. Increase in viscosity (shear thickening) occurs in the intermediate range of $\dot{\gamma}$ due to a shear-induced increase in the fraction of chains residing with hydrophobes in the cores of neighboring micelles, whereas reduction in viscosity (shear thinning) for high values of $\dot{\gamma}$ is the result of network fragmentation due the increase in the number of chains residing with both hydrophobes in the core of the same micelle.[4] In the latter regime, the mean number of hydrophobes per micelle core is conserved, and the number of micelles in solution does not change.

The amphiphilic and associative nature of the telechelic polymers leads to polymer adsorption in the form of multilayers on both hydrophilic and hydrophobic surfaces. Upon increase in polymer concentration in the vicinity of the substrate, the individual macromolecules undergo a sequence of transformations similar to that in the bulk solution and ultimately form a surface gel. (We stress that surface gelation may occur when no association or very limited association occurs in the bulk system.[5]) Adsorption of thick layers of associative polymers can change the properties of a bulk system, especially with a large surface area, increasing hydrodynamic dimensions of latex beads or bridging of colloid particles.[1a,6,7]

Adsorption of associative polymers and surface gelation also have an effect on time-dependent forces acting between the polymer-covered surfaces as they slide past each other.[8,9] Shear forces in polymer layers determine friction, wear, lubrication, and liquid flow past polymer-covered surfaces. The chemical structure and architecture of the constituent macromolecules, the extent of cross-linking, the degree of layer compression, the shear velocity, and polymer relaxation after shear are among the most important factors that govern friction properties of surface gels.

The surface force balance (SFB) with shear capability is a useful tool in studies of dynamic forces acting between adsorbed and/or confined polymer layers.[10] It has been successfully used to probe normal and shear forces acting between the surfaces bearing polymer monolayers (e.g., polymer brushes and adsorbed polymers[11−14]) and in confined polymer melts.[15,16] Eiser and Klein[17] and Kumacheva and Kim[18] employed the SFB technique to study the surface properties of telechelic polymers. The first group studied normal and shear forces in polymer brushes formed by telechelic polystyrene molecules end-terminated with small zwitterionic groups at both ends. This work focused on shear between the polymer monolayers; thus, loosely attached (associated) polymer was purposely removed by rapidly shearing compressed polymer-covered surfaces.[17] The second group reported properties of gelled telechelic polymer poly(ethylene oxide) end-capped with octadecyl groups at both ends.[18,19] This work, however, focused on normal forces acting between polymer-covered surfaces. It was found that above the critical micellization concentration, c_{cmc}, the telechelic polymer formed thick gel-like layers whose unperturbed thickness correlated with a hydrodynamic size of polymer micelles in the bulk solution. These findings agreed with the results of Russel et al.[7] obtained in studies of adsorption of the same polymer on latex particles.

10.1021/ma030453z CCC: $27.50
Published on Web 06/05/2004

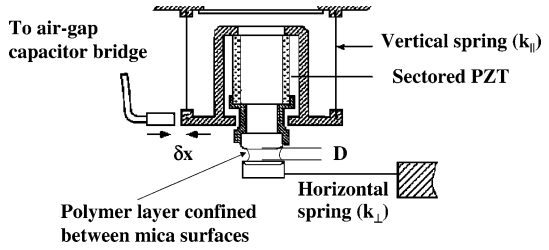

Figure 1. Schematic of the surface force balance used in the present study. Polymer is adsorbed to atomically smooth mica sheets mounted on the crossed cylindrical lenses. Lateral and normal displacements are provided by the piezo-electric tube (PZT) mounted on two orthogonal vertical leaf springs. The normal force is monitored via bending of the horizontal spring and measuring changes in D using multibeam interferometry. The shear force is measured by monitoring bending of the vertical spring δx, via changes in an airgap capacitor.

Here, our objective was to study shear forces acting between the surface gels formed by flexible telechelic polymer on hydrophilic substrates. We used poly(ethylene oxide) end-capped with alkyl groups at both ends, a polymer whose equilibrium surface properties were studied in earlier works.[7,18] The shear properties of adsorbed telechelic polymer were examined as a function of polymer concentration in solution, compression of adsorbed layers, and shear velocity. For weak and moderate polymer compression extremely weak shear forces were observed (below the resolution of the instrument); this effect was presumably caused by osmotic repulsion between poly(ethylene oxide) chains and shear thinning of the surface gel.

For strong confinement, the shear force showed a marked increase due to compression-forced interpenetration of the poly(ethylene oxide) backbones and interaction between hydrophobic groups.

Experimental Section

Materials. Poly(ethylene oxide) end-terminated with octadecyl groups with a formula

$$C_nH_{2n-1}-NH-CO-(OCH_2CH_2)_x-O-CO-NH-C_nH_{2n-1}$$

where $x = 800$ and $n = 18$ was synthesized at Rohm and Haas Co. The end-termination of poly(ethylene oxide) (MW = 35 000 g/mol, PDI = 1.2) and the purification of ODU-35K are described elsewhere.[7,20] Herein, we refer to the telechelic polymer as to ODU-35K.

To screen long-range electrostatic double-layer interactions, the normal force profiles were measured across the solutions of ODU-35K in 0.1 M solution of KNO_3. Since all ODU-35K solutions contained the same concentration of KNO_3, here we simply refer to them as to "polymer solutions". Polymer solutions were equilibrated for least 24 h prior to introduction into the SFB.

Potassium nitrate (purity >99.99%) was purchased from Sigma-Aldrich Canada Ltd. The deionized water was double-distilled prior to solution preparation. Ethanol and toluene (Fisher Inc.) used for cleaning of the glassware and of the different parts of the SFB were HPLC grade and spectroscopic grade (99.5%), respectively. Mica was first grade muscovite mica purchased from S&J Trading.

Methods. The design of the SFB apparatus with shear capability used in the present work is described elsewhere.[12,21] Two back-silvered mica sheets were mounted opposite each other onto a horizontal flexible leaf spring (bottom surface) and onto a four-sectored piezoelectric tube PZT (top surface) (Figure 1). The normal force, F_n, acting between the polymer layers adsorbed and confined between the surfaces was measured as $F_n = k_\perp \Delta D$, where ΔD is the deflection of a flexible horizontal leaf spring and $k_\perp = 70$ N/m is the spring constant. The bending of the spring was measured using an interferometric technique. The normal force was related to the interaction energy per unit area between the two flat surfaces using the Derjaguin approximation as $F_n/R = 2\pi E(D)$, where E is the free energy of interaction per unit area between the two flat surfaces, D is the distance between the surfaces, and R is the local mean radius of curvature of the surfaces.[22] The results of experiments were presented as the normalized force−distance profiles F_n/R vs D. A typical error in the measurements of normal forces did not exceed 15%.

To measure the shear forces acting between the surfaces, oscillatory back-and-forth lateral motion was applied to the upper surface. The shear velocity varied from 30 to 700 nm/s by changing the shear amplitude, A, and/or the shear frequency, f, using TTi TG 1010 (Thurlby Thandar Instruments) function generator. The shear force, F_s, in the polymer layer was measured as $F_s = k_{II}\delta x$, where $k_{II} = 200$ N/m is the spring constant of the vertical spring rigidly coupled to the top surface and δx is the spring bending measured with an air gap capacitor Accumeasure 9000 (MTI instruments Inc.).[10] The shear traces were recorded using a digital oscilloscope (Tektronix TDS 3012B). The sensitivity in measurements of shear forces was limited by ambient vibrations; thus, to minimize mechanical noise, an active antivibrational stage (MOD-1, Gottingen, Germany) was used. The resolution in measuring shear forces was $\delta F_s = \pm 0.2\ \mu$N.

In a typical SFB experiment, after measuring the contact position between the bare mica surfaces in air, verifying the purity of mica surfaces by measuring normal force−distance profiles in 0.1 M KNO_3 solution, and comparing them with the electrostatic double-layer overlap repulsion expected from the DLVO theory for 1:1 electrolyte 0.1 M solution,[22] the solution of KNO_3 was replaced with a polymer solution. The normal and shear force measurements were conducted following 18 ± 1 h surface exposure to the polymer solution. We report herein the results of four independent experiments.

The hydrodynamic radius, R_h, of micelles of ODU-35K was measured using photon correlation spectroscopy (DynoPro MS800, Protein Solutions). The diffusion coefficient, D, of micellar aggregates was related to their hydrodynamic radius through Stokes' equation as $D = k_BT/6\pi\eta_sR_h$, where k_B is the Boltzmann constant, T is the absolute temperature of the solution, and η_s is the viscosity of the solvent. All ODU-35K solutions were prepared in 0.1 M KNO_3 solutions.

Table 1. Hydrodynamic Radii of Polymer Micelles in Solutions of ODU-35K

C_{pol}, g/mL	R_h, Å	R_h[a] (PEO), Å
1.3×10^{-4}	185	61
0.9×10^{-4}	200	
0.5×10^{-4}	179	
0.2×10^{-4}	n/a	

[a] Obtained by Chassenieux et al.[34]

Results

Bulk Polymer Solutions. Table 1 shows the average hydrodynamic radii of polymer aggregates in solutions of ODU-35K. (As a reference system, we show the radius of gyration of a nonmodified PEO molecule with molecular weight 35000 g/mol.) Following dilution from 1.3×10^{-4} to 0.5×10^{-4} g/mL, the size of polymer associates underwent insignificant size change. Because of the lack of sensitivity of the instrument for $c_{pol} = 0.2 \times 10^{-4}$ g/mL, the dimensions of individual macromolecules were not measured.

Normal Forces. Figure 2 shows the repulsive force−distance profiles measured on the first approach of the mica surfaces equilibrated in 0.2×10^{-4}, 0.5×10^{-4}, and 1.3×10^{-4} g/mL ODU-35K solutions. (Repulsion forces measured in polymer-free 0.1 M KNO_3 solution

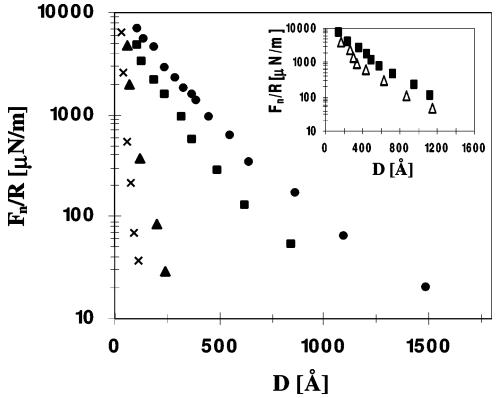

Figure 2. Equilibrium normalized force−distance profiles measured upon compression of the mica surfaces exposed to 0.1 M KNO_3 solution (×) and to ODU-35K solutions at c_{pol}, g/mL: 0.2×10^{-4} (▲), 0.5×10^{-4} (■), and 1.3×10^{-4} (●). The time of exposure is 18 ± 1 h. Inset: normal force−distance profiles between ODU-35K layers measured in compression (■) and rapid decompression cycle (△), $c_{pol} = 1.3 \times 10^{-4}$ g/mL.

commenced at $D = 150$ Å, consistent with our previous results reported in ref 18.) When c_{pol} increased, the surface separation at which repulsion commenced shifted toward larger distances. First, a strong increase in the force onset (from 300 to 1100 Å) occurred when polymer concentration increased from 0.2×10^{-4} to 0.5×10^{-4} g/mL. A more gradual shift in the onset of repulsion to 1600 Å occurred when c_{pol} was increased to 1.3×10^{-4} g/mL. The magnitude of repulsion force between the surfaces showed the same trend. The force profiles measured on compression and rapid decompression of the polymer-covered surfaces are shown in the inset to Figure 2. Weak force hysteresis is apparent from the shift of the decompression force profile toward shorter distances. The original force profile was measured after equilibration of the polymer layer for several hours. The results of normal force measurements and photon correlation spectroscopy (PCS) experiments were in agreement with our previous findings:[18] for $c_{pol} = 0.2 \times 10^{-4}$ g/mL the short force−distance range corresponded to repulsion between the monolayers of ODU-35K (resembling the repulsive forces between the monolayers of PEO with close molecular weight), whereas for $c_{pol} \geq 0.5 \times 10^{-4}$ g/mL, thick polymer layers adsorbed from micellar polymer solutions.

Shear Forces. Following normal force measurements, we examined the shear forces acting between the adsorbed layers of ODU-35K by applying back-and-forth lateral displacement to the top surface. The shear experiments were carried out only for thick gelled polymer layers, i.e., for $c_{pol} \geq 0.5 \times 10^{-4}$ g/mL. Shear force measurements were conducted for a different extent of compression of the polymer layer under different shear velocities.

Effect of Compression. The shear measurements commenced at large surface separations substantially exceeding the onset of normal forces between the surfaces. The experiments were conducted in two ways: (a) the surfaces were slowly approached under oscillatory shear, or (b) the surfaces were brought together to a particular surface separation D without shear, then shear was applied, the surfaces were separated, equilibrated for several hours, and the shear cycle was repeated. In both cases, the characteristic features of the shear behavior of adsorbed ODU-35 were similar.

In Figure 3 the top traces show a periodic displacement $\Delta x_0(t)$ applied to the top surface, leading to its

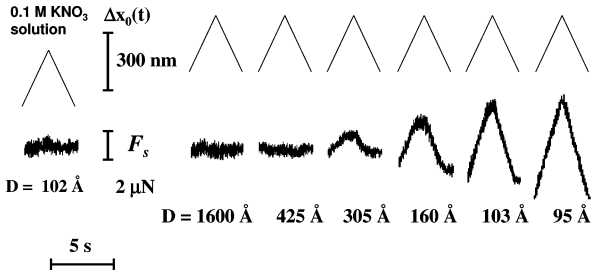

Figure 3. Shear traces recorded for ODU-35K layers adsorbed from polymer solution at $c_{pol} = 0.5 \times 10^{-4}$ g/mL at different surface separations D. The top traces show the back-and-forth lateral motion applied to the upper surface as a function of time; the bottom traces show the shear response translated to the lower surface. Only one period of the shear response at each separation is shown. Control shear experiments conducted in polymer-free 0.1 M electrolyte solution at $D = 102$ Å revealed that no shear stress was transmitted to the bottom surface.

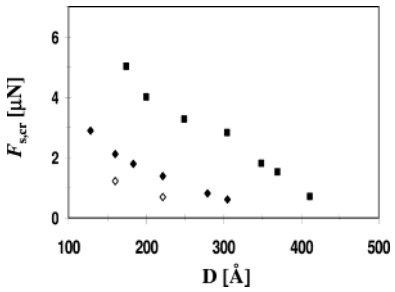

Figure 4. Variation in critical shear force extracted from its plateau value in shear traces (as in Figure 2) as a function of surface separation D for the polymer layers adsorbed from 0.5×10^{-4} (◆) and 1.3×10^{-4} g/mL (■) ODU-35K solutions. Shear velocity $v_s = 30$ nm/s. Filled symbols: polymer layers were sheared for $t < 30$ s; open diamonds: polymer layers adsorbed from 0.5×10^{-4} g/mL solutions were sheared for 120 s.

uniform back-and-forth lateral motion. The bottom traces show the variation in the shear force, F_s, generated in the layer. Upon progressive surface confinement (from left to right) the shear traces changed, reflecting the change in the shear properties of the polymer layer.

From large surface separations where no normal forces were observed down to $D \approx 425$ Å, no shear response distinguishable from the mechanical vibrations was detected. For surface separation $D = 425 \pm 10$ Å, the mechanical noise somewhat decreased; however, no shear response was noticed above the noise level. For $D = 305 \pm 10$ Å the first indication of the shear force in the layer was obtained. Then, from $D \approx 305$ Å down to $D \approx 103$ Å, the bottom traces featured an initial strong increase in the shear force followed by a plateau region, corresponding to sliding of the polymer-coated surfaces. The magnitude of the shear force, $F_{s,cr}$, corresponding to the plateau value increased with polymer compression. For $D < 103$ Å the response of the layer changed qualitatively: over the time scale of experiment the shear trace followed the change in lateral displacement of the top surface; that is, the plateau was not developed (Figure 3, right bottom trace).

Figure 4 shows the variation in $F_{s,cr}$ at different surface separations when the polymer layers were sheared for 30 s. (We note that only shear traces in which a plateau region in the shear force was reached could be used for extracting any useful information about the shear properties of the layer.) For the layers formed from 0.5×10^{-4} g/mL polymer solutions the shear force was below the resolution of the SFB for D

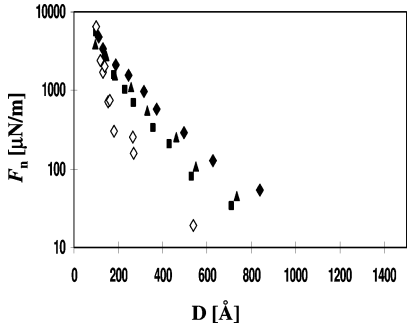

Figure 5. Normalized force−distance profiles measured prior to shear (◆) and immediately after shear run carried out under confinement $D = 320$ Å (■) and $D = 150$ Å (◇). $v_s = 60$ nm/s, $t = 30$ s. The normal force profile measured after compression without shear is given for comparison (▲).

> 305 Å, whereas from 305 to 128 Å the magnitude of $F_{s,cr}$ gradually increased from 0.5 to 2.9 μN (Figure 4, filled diamonds). In several measurements long-time shear ($t >$ 90 s) was applied for $D = 292$ Å and $D = 160$ Å (Figure 4, open diamonds), which led to a notable reduction of $F_{s,cr}$.

A qualitatively similar shear response was observed for ODU-35K adsorbed from 1.3×10^{-4} g/mL solution. When oscillatory lateral motion was applied to the polymer layer, from large surface separation exceeding $D = 1600$ Å (at which the normal repulsive force commenced) to ca. 575 Å no shear force in the layer above mechanical noise was resolved. For 575 ± 10 Å the mechanical vibrations significantly reduced. The shear force between the surfaces became measurable for $D \leq 420$ Å. For $160 < D < 420$ Å the critical shear force gradually increased to have the magnitude of up to ca. 5 μN, and for $D < 150$ Å the surfaces were practically coupled through a rigid polymer layer. The variation in $F_{s,cr}$ is shown in Figure 4 (filled squares). The distance range and the magnitude of $F_{s,cr}$ for the polymer layers are substantially larger than for those formed in the 0.5×10^{-4} g/mL solution.

Normal Forces following Shear. The force−distance profiles measured after shear experiments were strongly influenced by polymer compression during shear, by the duration of shear experiments, and by the shear velocity. Figure 5 shows the normalized force profiles measured prior to and following shear experiments for the layers formed from 0.5×10^{-4} g/mL polymer solution. When the surfaces were compressed to $D \approx 320$ Å and sheared for 30 s, the subsequently measured normal forces commenced at $D_0 = 850$ Å (Figure 5, filled squares), in contrast to 1100 Å measured before shear. This force−distance range was similar to that measured immediately after the first compression (without shear), also given in Figure 5 (filled triangles). In both cases, a complete recovery of the layer occurred after ca. 3−4 h. The insignificant difference between these profiles indicated that no substantial polymer expulsion from the gap between the surfaces occurred during shear and that hysteresis in adsorbed ODU-35K was caused by the structural rearrangements in the polymer layer during shear and/or compression. However, when the polymer layer was compressed to $D = 150$ Å and then subjected to shear, the subsequently measured $F_n(D)$ profiles underwent a more marked shift inward, with onset commencing at $D_0 = 600$ Å (Figure 5, open diamonds). A complete recovery of the layer occurred only in ca. 18 h (for the gap between the surfaces ca. 1−2 mm).

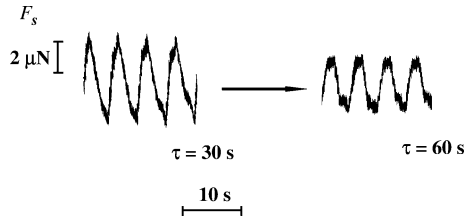

Figure 6. Variation in as-recorded oscilloscope shear traces for the polymer layers adsorbed from 1.3×10^{-4} g/mL ODU-35K solution following increase in shear duration. $D = 190$ Å, $A = 300$ nm, and $v_s = 60$ nm/s.

Effect of Long-Time Shear on Shear Forces. When the polymer-covered surfaces were sheared for a long time, e.g., exceeding 90 s, the magnitude of the shear force and sometimes the shape of the shear traces underwent changes. Figure 4 shows the first effect: when the ODU-35K layers were sheared with $v_s = 30$ nm/s for 120 s, the magnitude of the critical shear force changed from 2 to 1.2 μN ($D = 160$ Å) and from 1.3 to 0.7 μN ($D = 292$ Å).

The second effect is demonstrated in Figure 6. Polymer layers adsorbed from 1.3×10^{-4} g/mL ODU-35K solutions and compressed to $D = 190$ Å were sheared with $v_s = 60$ nm/s. Originally, the critical shear force corresponding to sliding (the plateau region of F_s) could not be extracted, suggesting that it was higher than 2.6 μN (Figure 6, left trace). After shear was applied for 60 s, a plateau appeared on the shear trace with $F_{s,c} = 1.7 \pm 0.2$ μN, shown in Figure 6, right trace. Additional decrease in $F_{s,c}$ could be observed when the shear velocity increased.

In the course of shear experiments, up to extremely strong confinement to $D = 80$ Å, for large shear amplitudes up to 600 nm, shear velocity up to 600 nm/s, and duration of shear up to 300 s, we have never observed that the polymer was completely removed from the gap between the surfaces and they came in contact.

Effect of Shear Velocity. The shear velocity, v_s, was varied by changing the amplitude or frequency of oscillatory lateral motion applied to the top surface (Figure 1). Since the structure of the polymer layer was sensitive to large shear amplitudes, here we show the results obtained by varying the shear frequency (keeping the amplitude at 300 nm). Figure 7a shows portions of the representative shear traces obtained for the layers adsorbed from polymer solution at $c_{pol} = 0.5 \times 10^{-4}$ g/mL. Following a 20-fold increase in v_s, all traces showed a typical region of rapidly increasing shear force for $F_s > F_{s,cr}$ and a plateau region corresponding to free sliding of the surfaces. All traces featured similar $F_{s,cr}$, which is further demonstrated in Figure 7b: for v_s varying from 30 to 600 nm/s the magnitude of $F_{s,cr}$ did not noticeably change. (A small increase in $F_{s,cr}$ for $v_s = 600$ nm/s was caused by the decrease in surface separation during shear from $D = 220$ to $D = 200$ Å.) Shear of ODU-35K layers adsorbed from 1.3×10^{-4} g/mL solution featured a similar trend.

In several experiments, shear with $v_s = 700$ nm/s led to decrease in the magnitude of $F_{s,cr}$. However, when shear with $v_s = 30$ nm/s was applied again, the original magnitude of the critical shear force was obtained, indicating that for moderate compression the shear response of the layer was reversible with respect to the variation in shear velocity.

For strong confinement, shear with large amplitudes resulted in changes similar to those shown in Figure 6:

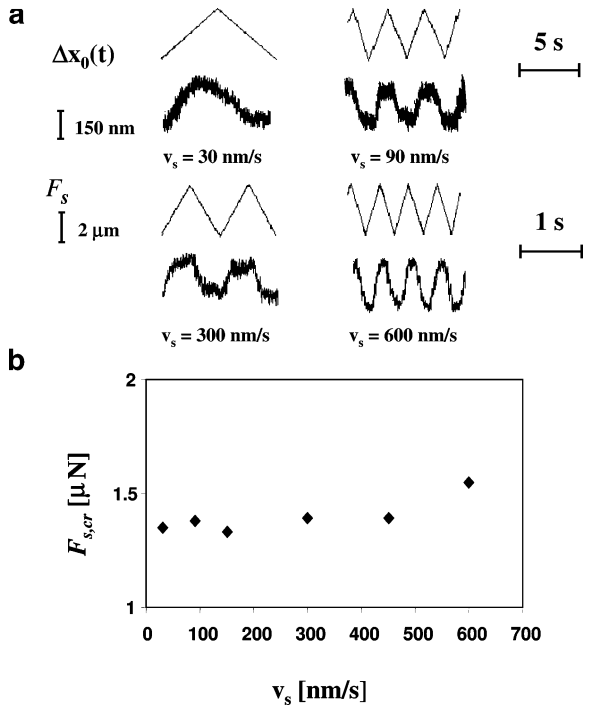

Figure 7. (a, top) Effect of shear velocity on shear of moderately compressed polymer adsorbed from 0.5×10^{-4} g/mL polymer solution and compressed to $D = 220$ Å. $t < 30$ s. Shear traces recorded for adsorbed polymer layers, at different shear velocities. (b, bottom) Variation in the critical shear force as a function of shear velocity. For $v_s = 600$ nm/s, the surfaces instantaneously moved to $D = 200$ Å.

it changed the shape of the shear traces from a "solid-like" response with no sliding to a sharp initial increase in the shear force followed by a clear plateau region indicative of sliding. The original shear response was obtained only after long-time equilibration of the polymer layer.

Discussion

It is crucial to analyze the surface properties of ODU-35K molecules in conjunction with their properties in the bulk solution in the range of c_{pol} studied. Using the photon correlation spectroscopy technique, we were unable to determine the size of individual macromolecules of ODU-35K for $c_{pol} = 0.2 \times 10^{-4}$ g/mL; however, this concentration was, clearly, below $c_{cmc} \approx 0.4 \times 10^{-4}$ g/mL, determined for ODU-35K by static fluorescence.[23,24] Two other concentration regimes studied were above c_{cmc}. The average hydrodynamic diameter of ODU-35K micelles of ca. 380 Å was close to ca. 420 Å reported by Russel et al.[20] for the same polymer. Polymer dilution to $c_{pol} = 0.5 \times 10^{-4}$ g/mL did not noticeably changed the average size of micelles. Thus, it was concluded that polymer adsorption in both concentration regimes occurred from the micellar solutions.

In the surface forces experiments, the onset of long-range osmotic repulsion, D_0, gave approximately the thickness, L, of the polymer layer adsorbed on each surface ($L = D_0/2$). For the surfaces exposed to 0.2×10^{-4} g/mL polymer solution the onset of repulsive interaction at $D_0 = 300$ Å suggested that following 18 ± 1 h adsorption the telechelic polymer formed a 150 Å thick monolayer, close to ca. 170 Å obtained in our earlier work for ODU-35K[18] and to ca. 140 Å measured for poly(ethylene oxide) end-terminated with dodecyl groups adsorbed at $c_{pol} < c_{cmc}$.[25] Thus, we conclude that when ODU-35K molecules existed as unimers in the bulk solution, the equilibrium surface structure was a monolayer, despite the associative nature of the polymer.[26]

The absence of attraction on approach of the polymer layers adsorbed on the opposite surfaces shed light on the conformation of macromolecules on the surface. Attraction could be expected between the dangling bridging groups exposed to the aqueous phase. For example, weak attraction was observed for telechelic polystyrene brushes end-capped with small zwitteronic groups, which were physically grafted to mica from toluene solution.[17] In contrast, in the present work the polymer layer had a more compact structure: poly(ethylene oxide) backbone adsorbed to the hydrophilic mica surface and the hydrophobic octadecyl groups were presumably hidden inside the layer (to avoid unfavorable contacts with water or hydrophilic mica).

A significant increase in the layer thickness L occurred for $c_{pol} > c_{cmc}$ ($c_{pol} \geq 0.5 \times 10^{-4}$ g/mL). (Adsorbed layers of telechelic polymers in selective solvents show a trend to thicken due to the associative nature of these polymers.) The equilibrium thickness of the polymer layer of $L = 550$ Å was in agreement with adsorption of 380 Å large ODU-35K micelles on the top of 150 Å thick monolayer. However, this oversimplified picture did not take in account the polydispersity of ODU-35K micelles[20] adsorption of individual macromolecules and the interactions between the micelles in the adsorbed layer. Indeed, following adsorption of micelles, a "loop-to-bridge" transition of macromolecules originally residing with two hydrophobes in the same micelle led to the formation of a two-dimensional physical gel, in which the macromolecules linked two neighboring micelles. Because of the local increase in polymer concentration on the substrate, surface gelation occurred at polymer concentrations significantly lower than $c_{pol} \approx 10^{-3}$ g/mL observed in bulk polymer solution.

Since the magnitude of repulsive forces driven by osmotic repulsion is directly related to the mean monomer concentration in the gap between the surfaces, we estimated the equilibrium adsorbance of ODU-35K using the equation[27]

$$\{F(D_1) - F(D_2)\}/R = -2\pi k_B N_A T/v_1\{(D_2 - 2\Gamma v) \ln(1 - 2\Gamma v/D_2) - (D_1 - 2\Gamma v) \ln(1 - 2\Gamma v/D_1) + \chi(2\Gamma v)^2(1/D_1 - 1/D_2)\}$$

derived for strong polymer confinement where Γ is equilibrium polymer adsorbance, $F(D_1)$ and $F(D_2)$ are equilibrium normal forces at distances D_1 and D_2, R is the radius of curvature of the surfaces, k_B is the Boltzmann constant, N_A is the Avogadro number, T is the temperature, v_1 is the molar volume of water (18 cm^3/mol), v is the specific volume of poly(ethylene oxide) ($v = 0.89$ cm^3/g), and χ is the water−PEO segment interaction parameter ($\chi = 0.47$).[28]

Using the experimental data, we found that equilibrium polymer adsorbance was 1.7 ± 0.1, 6.0 ± 1.3, and 8.1 ± 1.7 mg/m^2 for $c_{pol} = 0.2 \times 10^{-4}$, 0.5×10^{-4}, and 1.3×10^{-4} g/mL, respectively, reasonably close to equilibrium adsorbance of ODU-35K obtained on the basis of refractive index measurements.[18]

The main finding of this work is a very low magnitude of shear force in the moderately compressed polymer layers. This effect is clearly shown in Figure 8, in which

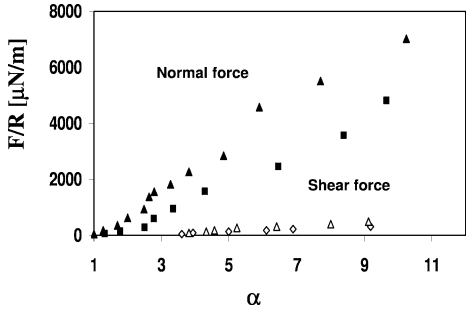

Figure 8. Variation in normalized normal (●, ◆) and critical shear force (○, ◇) as a function of extent of polymer layer compression, $\alpha = 2L/D$, where $L = D_0/2$ is found from the equilibrium normal force−distance profile. Triangles: $c_{pol} = 1.3 \times 10^{-4}$ g/mL; circles: $c_{pol} = 0.5 \times 10^{-4}$ g/mL. $v_s = 30$ nm/s.

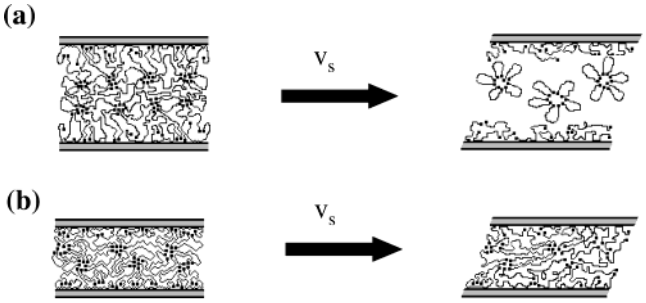

Figure 9. Schematic illustration of the structure of the sheared surface gel under moderate (a) and strong (b) compression (see text).

both normal and shear forces (normalized by the surface radius of curvature R) are plotted vs surface compression ratio, α, defined as $\alpha = 2L/D$ ($=D_0/D$). For $c_{pol} = 0.5 \times 10^{-4}$ g/mL the first detectable shear response appeared when the polymer layer was compressed to $\alpha \approx 3.6$ ($D = 305$ Å, $D_0 = 1600$ Å). Similarly, for the ODU-35K layer adsorbed from 1.3×10^{-4} g/mL polymer solution, the first measurable shear force was obtained for $\alpha = 3.8$ ($D = 420$ Å, $D_0 = 1100$ Å). We note that the normal repulsion forces became apparent for $\alpha = 1$ and upon further compression had a much higher magnitude.

We ascribe a very low magnitude of friction force in the moderately compressed polymer layers to osmotic repulsion of PEO fragments and shear thinning of the micellar gel: for $1 < \alpha < 3.7 \pm 0.1$ and $v_s = 30$ nm/s, the surfaces slid on top of each other through a fluidlike layer, as shown schematically in Figure 9a. In this surface separation range, shear-induced removal of the loosely attached polymer from the gap between the surfaces was unlikely: hysteresis in the normal forces measured before and after shear was very similar to hysteresis observed in a compression−decompression cycle without shear (Figure 6a). A similar shear-induced fragmentation of the bulk network structure above the critical shear rate was observed by several groups.[29−31] The micellar gel yielded and the telechelic chains underwent bridge-to-loop transitions yielding individual micelles.

For strong layer compression $\alpha > 3.7 \pm 0.1$ an increase in interpenetration and entanglement of the macromolecules adhering to the two opposite surfaces and compression-forced interactions between the octadecyl groups (Figure 9b) led to increase in viscous dissipation in the polymer layer and, as a result, to a graduate increase in $F_{s,cr}$. Further compression (down to ca. 10% of the original thickness) led to a slow

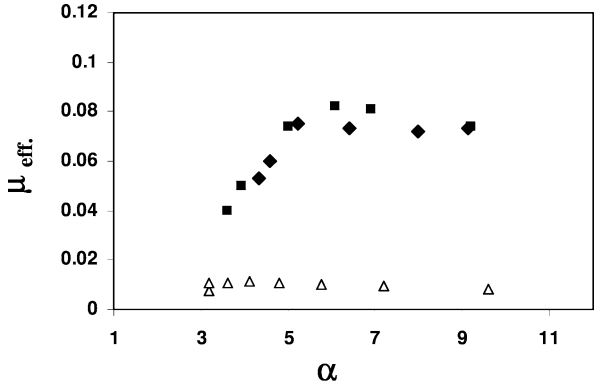

Figure 10. Variation of the effective kinetic friction coefficient μ_{eff} ($F_{cr,s}/F_n$) with extent of surface compression α for ODU-35K layers adsorbed from 0.5×10^{-4} g/mL solution (◆) and 1.3×10^{-4} g/mL solution (■). Values of $F_{s,cr}$ and F_n are taken from profiles in Figure 8. The variation in effective kinetic friction coefficient for PEO (MW = 112 000) monolayers adsorbed from toluene solution to mica surface (△) is adapted from Figures 4 and 14 in ref 13.

increase in the shear force, in contrast with rapid increase in normal forces, shown in Figure 8. Additional characterization of friction between the micellar surface gels was conducted by plotting the effective friction coefficient, $\mu_{eff} = F_{s,cr}/F_n$, as a function of compression ratio of the ODU-35K layers. The value of μ_{eff} for the sheared ODU-35K layers gradually increased from 0.03 to 0.072 for $3.6 < \alpha < 9.1$ ($c_{pol} = 0.5 \times 10^{-4}$ g/mL) and from 0.04 to 0.075 for $3.75 < \alpha < 9.2$ ($c_{pol} = 1.3 \times 10^{-4}$ g/mL). To extract the contribution of hydrophobic groups vs viscous dissipation between the rubbing PEO chains, we plotted the variation in μ_{eff} for the sheared monolayers of PEO (MW = 37 000) adapted from ref 13. Although PEO was adsorbed from toluene, a better solvent for this polymer than water (χ is 0.39 and 0.47 in toluene and water, respectively[32]), a qualitative conclusion can be made on the basis of such a comparison. For the PEO layers in the same range of compression ratios, the effective friction coefficient remained below 0.01. Second, the variation in effective friction coefficient for PEO layers scaled as $\mu_{eff} \propto D^{1/3}$ (or $\mu_{eff} \propto \alpha^{-1/3}$), whereas ODU-35K layers up to $\alpha \approx 6.5$ showed a more marked dependence of μ_{eff} vs α. A stronger shear response of the ODU-35K layers could be due to the interactions between the hydrophobic end groups and/or a more substantial interpenetration of the micellar gel layers upon compression.

In strongly compressed layers long-time shear and large sliding velocity (≥600 nm/s) led to the same effect: the defragmentation of the surface micellar gel and thus the reduction in shear forces. While for moderate surface compression such defragmentation was reversible and the surface gel rapidly restored its structure when v_s was reduced, under strong compression the recovery of the sheared layer was hindered.

A very weak velocity dependence of the shear force resulted from the decreasing interpenetration of the polymer layers (when shear velocity increased) and/or from the slip at the polymer−mica interface. (In the former case, increase in viscous dissipation in the interpenetration zone between the polymer layers was compensated by the smaller zone thickness.[13]) The transition from the first to the second regime was possible, as follows from Figure 10: increase in surface compression ratio α could shift the slip plane to the polymer−substrate surface.

In conclusion, we have conducted a study of frictional forces between the adsorbed layers of associative polymer poly(ethylene oxide) end-capped with octadecyl groups. The micellar surface gels of this telechelic polymer showed a complicated behavior dependent on the extent of the layer compression, the duration of the shear experiments, and the shear velocity. We found that under low pressures the surface gels showed very weak friction forces caused by polymer shear thinning. At high surface pressures the shear force increased. Compression of the polymer layers to ca. 27% of their original thickness led to increased frictional interactions between the surfaces, strongly influenced by the interactions between the hydrophobic groups. These results have at least two important implications for understanding and controlling the frictional properties of thermoreversible gels. First, shear thinning can be an important mechanism in biolubrication, since many biopolymers such as proteins and polysaccharides have an associative nature.[33] Second, to enhance lubrication, hydrophobic interactions between the nonpolar groups can be compensated by e.g. chemically modifying telechelic polymers with functional groups repelling each and thus reducing mutual interpenetration of the polymer macrochains upon compression.

Acknowledgment. The authors are grateful to Professor Rubinstein (University of North Carolina at Chapel Hill) for extremely helpful discussions. We also thank Professor Sheiko for his assistance in AFM imaging of the polymer layers. E.K. thanks ORCDF funding for financial support of this work.

References and Notes

(1) (a) Glass, J. E. In *Water-Soluble Polymers: Beauty with Performance*; Glass, J. E., Ed.; Advances in Chemistry 213; American Chemical Society: Washington, DC, 1986; p 391. (b) Karunasena, A.; Brown, R. G.; Glass, J. E. In *Polymers in Aqueous Media: Performance through Association*; Glass, J. E., Ed.; Advances in Chemistry 223; American Chemical Society: Washington, DC, 1989; p 495. (c) In *Hydrophilic Polymers*; Glass, J. E., Ed.; Advances in Chemistry 248; American Chemical Society: Washington, DC, 1996; p 449.
(2) *Industrial Water Soluble Polymers*; Finch, C. A., Ed.; The Royal Society of Chemistry: Cambridge, U.K., 1996.
(3) (a) Rubinstein, M.; Dobrynin, A. V. *Trends Polym. Sci.* **1997**, *5*, 181. (b) Winnik, M. A.; Yekta, A. *Curr. Opin. Colloid Interface Sci.* **1997**, *2*, 424.
(4) Tam, K. C.; Jenkins, R. D.; Winnik, M. A.; Bassett, D. R. *Macromolecules* **1998**, *31*, 4149.
(5) Kitaev, V.; Kumacheva, E. *Macromolecules* **2003**, *36*, 4924.
(6) Sperry, P. R.; Thibeault, J. C.; Konstanek, E. C. *Adv. Org. Coat. Sci. Technol.* **1987**, *9*, 1.
(7) Pham, Q. T.; Russel, W. B.; Lau, W. *J. Rheol.* **1998**, *42*, 159.
(8) Dan, N. *Curr. Opin. Colloid Interface Sci.* **1996**, *1*, 48.
(9) Gong, J. P.; Osada, Y. *Prog. Polym. Sci.* **2003**, *27*, 3.
(10) E.g., see review: Kumacheva, E. *Prog. Surf. Sci.* **1998**, *2*, 75.
(11) (a) Granick, S. *Langmuir* **1996**, *12*, 4537. (b) Klein, J.; Kumacheva, E.; Perahia, D.; Fetters, L. *J. Acta Polym.* **1998**, *49*, 617.
(12) Klein, J.; Kumacheva, E.; Perahia, D.; Mahalu, D.; Warburg, S. *Faraday Discuss.* **1994**, *98*, 173.
(13) Raviv, U.; Tadmor, R.; Klein, J. *J. Phys. Chem. B* **2001**, *105*, 8125.
(14) Raviv, U.; Frey, J.; Sak, R.; Laurat, P.; Tadmor, R. Klein, J. *Langmuir* **2002**, *18*, 7482.
(15) (a) Luengo, G.; Schmitt, F. J.; Hill, R.; Israelachvili, J. *Macromolecules* **1997**, *30*, 2482. (b) Luengo, G.; Heuberger, M.; Israelachvili, J. *J. Phys. Chem. B* **2000**, *104*, 7944.
(16) Kojio, K.; Jeon, S.; Granick, S. *Eur. Phys. J. E* **2002**, *8*, 167.
(17) Eiser, E.; Klein, J. *Phys. Rev. Lett.* **1999**, *82*, 5076.
(18) Kim, H. S.; Lau, W.; Kumacheva, E. *Macromolecules* **2000**, *33*, 4561.
(19) Extensive studies of poly(ethylene oxide) end-terminated with hydrophobic groups at both ends indicate that this polymer forms thermoreversible gels in bulk solutions (see e.g. ref 3 and references therein). In particular, ODU-35K forms a gel at c_{pol} just below 1 wt %. In our experiments c_{pol} in the gap between the surfaces (obtained from polymer absorbance) was about 4−9 wt %, that is, well above the threshold of gelation.
(20) Pham, Q. T.; Russel, W. B.; Thibeault, J. C.; Lau, W. *Macromolecules* **1999**, *32*, 2996.
(21) Klein, J.; Kumacheva, E. *J. Chem. Phys.* **1998**, *108*, 6996.
(22) *Surface Forces*; Derjaguin, B. V., Churaev, N. V., Kitchener, J. A., Muller, V. M., Eds.; Consultants Bureau: New York, 1987.
(23) Vorobyova, O.; Lau, W.; Winnik, M. A. *Langmuir* **2001**, *17*, 1357.
(24) We were able, however, to measure hydrodynamic diameter of poly(ethylene oxide) molecules end-terminated with C8H15 groups. This polymer undergoes association at its higher concentration, which allowed us to exceed the threshold of the sensitivity of PCS. For MW = 35 000 the hydrodynamic diameter of individual molecules was 136 Å.
(25) Ouali, L.; Francois, J.; Pefferkorn, E. *J. Colloid Interface Sci.* **1999**, *215*, 36.
(26) The absence of surface micelles of ODU-35K in polymer solutions at $c_{pol} < c_{cmc}$ has been proved in AFM experiments.
(27) Klein, J.; Luckham, P. F. *Macromolecules* **1984**, *17*, 1041.
(28) Brandrup, J., Immergut, E. H., Eds.; *Polymer Handbook*, 3rd ed.; Wiley: New York,, 1989.
(29) Ma, S. X.; Cooper, S. L. *Macromolecules* **2001**, *34*, 3294.
(30) Xu, B.; Yekta, A.; Li, L.; Masoumi, Z.; Winnik, M. A. *Colloids Interfaces A* **1996**, *112*, 239.
(31) Pham, Q. T.; Russel, W. B.; Thibeault, J. C.; Lau, W. *Macromolecules* **1999**, *32*, 5139.
(32) We admit that the change in χ-parameter of PEO may occur in 0.1 M KNO_3 solution.
(33) (a) Morris, E. R. *Carbohydr. Polym.* **1990**, *13*, 85. (b) Cui, W.; Kenaschuk, E.; Mazza, G. *Food Hydrocolloids* **1996**, *10*, 221. (c) Cassin, G.; Heinrich, E.; Spikes, H. A. *Tribol. Lett.* **2001**, *11*, 95.
(34) Chassenieux, C.; Nicolai, T.; Durand, D. *Macromolecules* **1997**, *30*, 4952.

MA030453Z